The properties of low-lying levels in ^{37}Cl (populated in $^{34}S(\alpha,p\gamma)$ reaction)

1974 J. Phys. A: Math. Nucl. Gen. 7 1437

(http://iopscience.iop.org/0301-0015/7/12/006)

J. Phys. A: Math., Nucl. Gen., Vol. 7, No. 12, 1974. Printed in Great Britain. © 1974

The properties of low-lying levels in ^{37}Cl

P J Nolan, L L Gadeken†, A J Brown, P A Butler, L L Green,
A N James, J F Sharpey-Schafer and D A Viggars‡

Oliver Lodge Laboratory, University of Liverpool, PO Box 147, Liverpool L69 3BX, UK

Received 24 January 1974, in final form 5 March 1974

Abstract. Excitation energies, mean lifetimes, gamma-ray branching ratios, angular correlations and linear polarizations have been measured for levels below 5·3 MeV in ^{37}Cl. The states were populated using the ^{34}S(α, pγ)^{37}Cl reaction at bombarding energies between 9·0 MeV and 12·2 MeV. A gamma–gamma coincidence experiment was performed at 11·5 MeV to obtain the decay scheme. New measurements were made for the following levels: $E_x(\tau_m)J^\pi$; 3087 keV (<40 fs) $\frac{5}{2}^+$; 3105 keV (48 ± 5 ps) $\frac{7}{2}^-$; 3626 keV (40 ± 20 fs) $\frac{3}{2}$, $\frac{5}{2}$, $\frac{7}{2}^+$; 3708 keV (<25 fs) $\frac{3}{2}^+$, $\frac{5}{2}^-$; 3740 keV (<20 fs) $\frac{5}{2}^-$; 4011 keV (31 ± 3 ps) $\frac{9}{2}^-$; 4547 keV (2·7 ± 0·6 ps) $\frac{11}{2}^-$ and 5271 keV (2·7 ± 0·4 ps) $\frac{13}{2}^-$. The results are compared with the properties of high-spin negative-parity states in neighbouring nuclei and are discussed in terms of recent shell-model calculations.

1. Introduction

The low-lying levels of ^{37}Cl have been investigated as part of a systematic study of nuclei in the upper region of the s–d shell. Before this work very little was known about ^{37}Cl as has been pointed out by Endt and van der Leun (1974). Previous measurements have established the mean lifetimes of the first two excited states and made definite spin and parity assignments for three of the eight levels below 5 MeV. These results are derived from various reactions, ^{36}S(p, γ)^{37}Cl (Harris and Perizzo 1970, Hyder *et al* 1969), ^{34}S(α, pγ)^{37}Cl (Alenius *et al* 1972), ^{37}Cl(p, p′γ)^{37}Cl (Duncan *et al* 1969), ^{37}Cl (n, n′γ)^{37}Cl (Nichols *et al* 1966) and a study of the β decay of ^{37}S (Klotz and Walter 1973). We have used the ^{34}S(α, pγ)^{37}Cl reaction to investigate in more detail the properties of levels below 5·3 MeV excitation. Recent measurements in the upper region of the s–d shell have shown that the high-spin negative-parity states in ^{29}Si can be well represented by the simple rotational model (Viggars *et al* 1973), while in ^{37}Ar they can be explained by the core-excitation model (Gadeken *et al* 1974). The high-spin negative-parity states in ^{37}Cl cannot however be explained by either of these models or the simple shell-model calculations available at present (eg Erné 1966).

2. Experimental method and data analysis

The states in ^{37}Cl were populated using the ^{34}S(α, pγ)^{37}Cl (Q = 3·03 MeV) reaction. The decay scheme was derived from a gamma–gamma coincidence experiment, using two large Ge(Li) detectors, at an alpha-particle bombarding energy of 11·5 MeV. The details of this experiment have been described by Gadeken *et al* (1974). The targets

† Present address: Department of Physics, Queens University, Kingston, Ontario, Canada.
‡ Present address: AERE Harwell, Berkshire, UK.

for all the present experiments were CdS, the sulphur content being enriched to 90% ^{34}S. For all measurements the gamma-ray detectors were calibrated for energy and efficiency using the known gamma-ray energies and relative intensities of a ^{56}Co source (Camp and Meredith 1971).

2.1. Doppler shift attenuation method (DSAM), *angular correlation and linear polarization measurements*

The apparatus and method of data analysis have been described previously by Butler *et al* (1973) and Gadeken *et al* (1974). The three types of measurements were taken simultaneously for alpha-particle bombarding energies of 9·0 MeV (DSAM only), 9·5 MeV, 10·5 MeV and 11·5 MeV at angles of 0°, 30°, 45°, 60° and 90°. For the 9·0 MeV and 9·5 MeV runs measurements were also taken at 110° and 125°, while at 11·5 MeV 38° and 52° were added to the original five angles. In the angular correlation experiments the gamma-ray angular distributions were normalized to the isotropic angular distribution from the 1410 keV $\frac{1}{2}^+ \rightarrow \frac{3}{2}^+$ transition in ^{37}Ar. The $\frac{1}{2}^+$ level is populated at the same time in the ^{34}S(α, nγ)^{37}Ar reaction. In fitting the data the angular correlation experiments, the experimental linear polarizations and also the predictions of the statistical compound-nucleus reaction model for the substate populations have been used to form a sum of squares of residuals. This is then minimized as a function of the mixing ratio in the usual manner. This procedure has been described in detail by James *et al* (1974), who also describe the procedure we have used in assigning the error limits on the mixing ratios.

2.2. Recoil distance method (RDM) *measurements*

The apparatus and the method of data analysis have been described previously by Nolan *et al* (1973). Measurements were taken at bombarding energies of 9·6 MeV, 10·4 MeV, 11·1 MeV and 12·2 MeV for the 3105 keV, 906 keV, 536 keV and 724 keV gamma rays respectively. These energies were chosen so that the level of interest was not being fed by a decay from a higher level. A different target was used for each run, their thicknesses being in the range 40 to 70 μg cm^{-2} CdS deposited onto 2 to 3 mg cm^{-2} gold foils. The stopper was a 6 mg cm^{-2} gold foil, this is sufficiently thick to stop the recoiling ^{37}Cl nuclei while the beam passes through, to a gold backstop, losing 10–15% of its energy. It was found necessary to use a foil stopper to reduce the heating effects of the beam.

The intensities of the stopped and shifted peaks from the 3105 keV transition could not be extracted using the peak shape fitting procedure described by Nolan *et al* (1973) due to the presence of the shifted peak from the 3087 keV transition ($\tau < 40$ fs). The following procedure has been used.

The centroid of the stopped and shifted peaks of the 3105 keV transition is given by

$$C_{12} = \frac{I_1 C_1 + I_2 C_2}{I_1 + I_2}$$

where the suffices 1 and 2 refer to the stopped and shifted peaks respectively and I and C refer to the intensity and centroid of the peaks. This becomes:

$$C_{12}(d) = A\,\mathrm{e}^{-d/d_{\mathrm{m}}} + B$$

where A and B are constants and d_{m} is the mean distance for decay. When a third peak is introduced the centroid of the multiplet is given by

$$C_T = \frac{I_{12}C_{12} + I_3C_3}{I_T}$$

where the suffix T refers to the multiplet. If I_3/I_T is constant and C_3 is independent of d (eg a transition with a short lifetime produced by the same reaction) the expression for C_T can be written

$$C_T(d) = D\,e^{-d/d_m} + E$$

where D and E are constants. Thus the centroid of the multiplet as a function of d can be used to find d_m without knowing the intensity I_3. Figure 1(a) shows the decay curve of the 3105 keV transition obtained using this procedure.

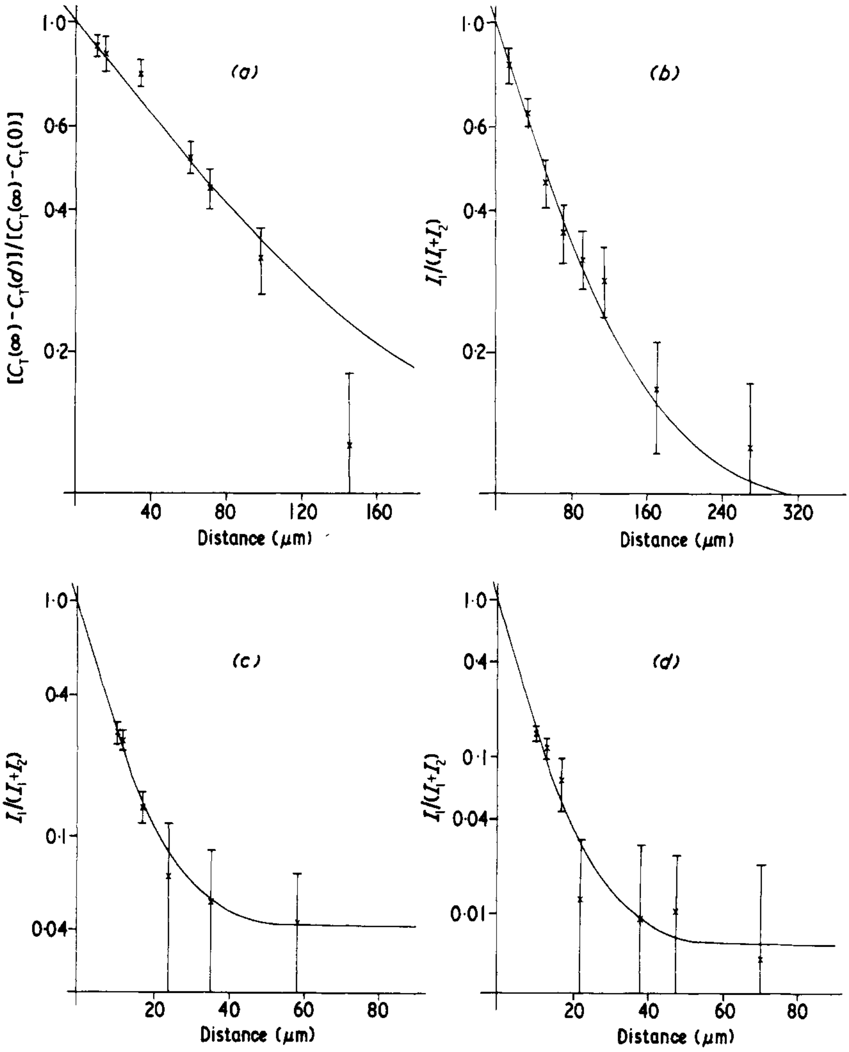

Figure 1. Decay curves used to determine the lifetimes of the following levels. (The 5 mm points are not shown.) (a) E_x = 3105 keV, E_γ = 3105 keV, d_m = 80 ± 8 μm, τ = 48 ± 5 ps; (b) E_x = 4011 keV, E_γ = 906 keV, d_m = 65 ± 7 μm, τ = 31 ± 3 ps; (c) E_x = 4547 keV, E_γ = 536 keV, d_m = 5·5 ± 0·8 μm, τ = 2·7 ± 0·6 ps; (d) E_x = 5271 keV, E_γ = 724 keV, d_m = 5·6 ± 0·4 μm, τ = 2·7 ± 0·4 ps. The symbols used in the diagram are explained in the text.

3. Results

The results presented here supercede a preliminary report on this work which appears in the proceedings of the Munich conference (Sharpey-Schafer *et al* 1973). The measured excitation energies, attenuation factors F and DSAM mean lifetimes are given in table 1. The procedure for converting F into the mean lifetime has been described by Gadeken *et al* (1974). The RDM mean lifetimes are given in table 2, while table 3 contains the measured angular correlation coefficients and linear polarizations. Table 4 contains the branching ratios, the mixing ratios and the transition strengths corresponding to all acceptable spin hypotheses for the initial level. Figure 2 shows the decay scheme derived from the present work.

Table 1. Measured energies, attenuation factors and DSAM mean lifetimes.

E_x (keV)	E_γ (keV)	E_α (MeV)	F	τ_m Present (fs ± 25%)†	τ_m Previous (fs)
1726·5 ± 0·3	1726·1 ± 0·4	9·0	0·63 ± 0·03	220 ± 25	230 ± 70‡
	1726·8 ± 0·4	9·5	0·61 ± 0·05		140 ± 60§
3086·6 ± 0·8	3086·5 ± 1·0	9·0	0·98 ± 0·04	< 40	66 ± 15‡
	3086·7 ± 1·0	9·5	0·96 ± 0·05		30 ± 12§
3105·0 ± 0·6	3104·9 ± 0·8	9·0	− 0·03 ± 0·01	> 3500	> 7000‡
	3105·1 ± 0·8	9·5	0·02 ± 0·04		> 1000§
3626·0 ± 0·6	3625·7 ± 0·7	10·5	0·95 ± 0·03	40 ± 20	
	3626·4 ± 0·8	11·5	0·90 ± 0·05		
3707·9 ± 0·6	3707·6 ± 0·7	10·5	0·97 ± 0·02	< 25	
	3708·2 ± 0·8	11·5	0·95 ± 0·02		
3740·5 ± 0·6	3740·7 ± 0·7	10·5	0·99 ± 0·01	< 20	
	3740·3 ± 0·8	11·5	0·96 ± 0·02		
4011·4 ± 0·2	4011·1 ± 0·8	10·5	< 0·01	> 4000	
	906·4 ± 0·2	10·5	0·02 ± 0·01		
4546·9 ± 0·3	535·5 ± 0·2	11·5	0·13 ± 0·03	2200 ± 700	
5271·2 ± 0·3	724·3 ± 0·2	11·5	0·17 ± 0·22	> 500	

† A 25% error is shown in the time scale as an indication of the uncertainties in the stopping theory.
‡ Duncan *et al* (1969).
§ Piiparnen *et al* (1973).

Table 2. Mean lifetimes obtained using the recoil distance method.

E_x (keV)	E_γ (keV)	E_α (MeV)	d_m (μm)	τ_m (ps)
3105	3105	9·6	80 ± 8	48 ± 5
4011	906	10·4	65 ± 7	31 ± 3
4547	536	11·1	5·5 ± 0·9	2·7 ± 0·6
5271	724	12·2	5·6 ± 0·4	2·7 ± 0·4

Table 3. Measured angular distribution coefficients and linear polarizations.

E_x (keV)	E_γ (keV)	Legendre coefficients† a_2	Legendre coefficients† a_4	Linear polarizations
3087	3087	+0·69 ± 0·02	+0·13 ± 0·03	−0·33 ± 0·28
3626	3626	+0·31 ± 0·05	−0·03 ± 0·06	−1·47 ± 0·78
3708	3708	−0·44 ± 0·04	−0·06 ± 0·05	+1·05 ± 0·40
3740	3740	−0·18 ± 0·02	−0·07 ± 0·03	+0·81 ± 0·29
4011	4011	+0·78 ± 0·04	+0·11 ± 0·04	+0·54 ± 0·28
	906	+0·70 ± 0·01	+0·19 ± 0·01	−0·95 ± 0·04
4547	536	−0·30 ± 0·01	0·00 ± 0·01	−0·49 ± 0·03
5271	724	−0·13 ± 0·02	−0·07 ± 0·02	−0·55 ± 0·10

† Normalized to $a_0 = 1$ and corrected for solid angle effects.

Table 4. Branching ratios, mixing ratios and transition strengths.

E_x (keV)	E_γ (keV)	Branching ratio (%)	$J_i^\pi \rightarrow J_f^\pi$	δ	Transition strengths: Electric (Wu)	Transition strengths: Magnetic (mWu)
1726	1726	100	$\frac{1}{2}^+ \rightarrow \frac{3}{2}^+$	†	33	30
3087	3087	100	$\frac{5}{2}^+ \rightarrow \frac{3}{2}^+$	−(1·6 ± 0·4)	> 5	> 5
3105	3105	100	$\frac{7}{2}^- \rightarrow \frac{3}{2}^+$	−(0·18 ± 0·01)‡	5·1 ± 1·1	(0·28 ± 0·03) × 10^3
3626	3626	100	$\frac{3}{2}^+ \rightarrow \frac{3}{2}^+$	−(2·5 ± 0·8)	4^{+4}_{-2}	2^{+6}_{-1}
			$\frac{3}{2}^+ \rightarrow \frac{3}{2}^+$	−(0·12 ± 0·09)	$0{\cdot}06^{+0{\cdot}35}_{-0{\cdot}05}$	16^{+16}_{-6}
			$\frac{3}{2}^- \rightarrow \frac{3}{2}^+$	−(0·12 ± 0·09)	$(5^{+5}_{-2}) \times 10^{-4}$	$(2^{+11}_{-2}) \times 10^3$
			$\frac{5}{2}^+ \rightarrow \frac{3}{2}^+$	$-(9^{+20}_{-4})$	5^{+5}_{-2}	$0{\cdot}2^{+1{\cdot}1}_{-0{\cdot}2}$
			$\frac{5}{2}^+ \rightarrow \frac{3}{2}^+$	−(0·41 ± 0·07)	$0{\cdot}6^{+1{\cdot}0}_{-0{\cdot}3}$	14^{+16}_{-5}
			$\frac{5}{2}^- \rightarrow \frac{3}{2}^+$	−(0·41 ± 0·07)	$(4^{+4}_{-1}) \times 10^{-4}$	$(23^{+37}_{-12}) \times 10^3$
			$\frac{7}{2}^+ \rightarrow \frac{3}{2}^+$	−(0·02 ± 0·07)	4^{+4}_{-1}	—
3708	3708	100	$\frac{3}{2}^+ \rightarrow \frac{3}{2}^+$	+(1·4 ± 0·8)	> 2·5	> 3·5
			$\frac{5}{2}^- \rightarrow \frac{3}{2}^+$	+(0·10 ± 0·05)	> 7 × 10^{-4}	> 0·5 × 10^3
3740	3740	100	$\frac{5}{2}^- \rightarrow \frac{3}{2}^+$	−(0·07 ± 0·03)	> 7 × 10^{-4}	> 0·4 × 10^3
4011	4011	31 ± 1	$\frac{9}{2}^- \rightarrow \frac{3}{2}^+$	0·00 ± 0·02	13 ± 1	—
	906	69 ± 1	$\frac{9}{2}^- \rightarrow \frac{7}{2}^-$	−(0·73 ± 0·04)	1·4 ± 0·2	0·6 ± 0·1
4547	536	100	$\frac{11}{2}^- \rightarrow \frac{9}{2}^-$	−(0·04 + 0·02)	$1{\cdot}5^{+3{\cdot}0}_{-1{\cdot}2}$	76 ± 18
	1442	< 5	$\frac{11}{2}^- \rightarrow \frac{7}{2}^-$	†	< 0·35	
5271	724	100	$\frac{13}{2}^- \rightarrow \frac{11}{2}^-$	−(0·07 ± 0·04)	$1{\cdot}0^{+2{\cdot}0}_{-0{\cdot}8}$	31 ± 5
	1260	< 5	$\frac{13}{2}^- \rightarrow \frac{9}{2}^-$	†	< 0·6	

† Not measured. Pure values have been calculated for the transition strengths.
‡ Measured by Hyder *et al* (1969).

3.1. The 1726 keV, 3087 keV and 3105 keV levels

The spin of the 1726 keV level is well established as $\frac{1}{2}^+$. Our mean lifetime of 220 ± 55 fs agrees with several previous measurements (eg Duncan *et al* 1969).

Alenius *et al* (1972) have shown the spin of the 3087 keV level to be $\frac{5}{2}$. The 3087 keV and 3105 keV levels form a doublet in the gamma-ray spectrum and at angles between 0° and 60° the 3087 keV gamma ray (τ < 40 fs) shifts into and is obscured by the 3105 keV

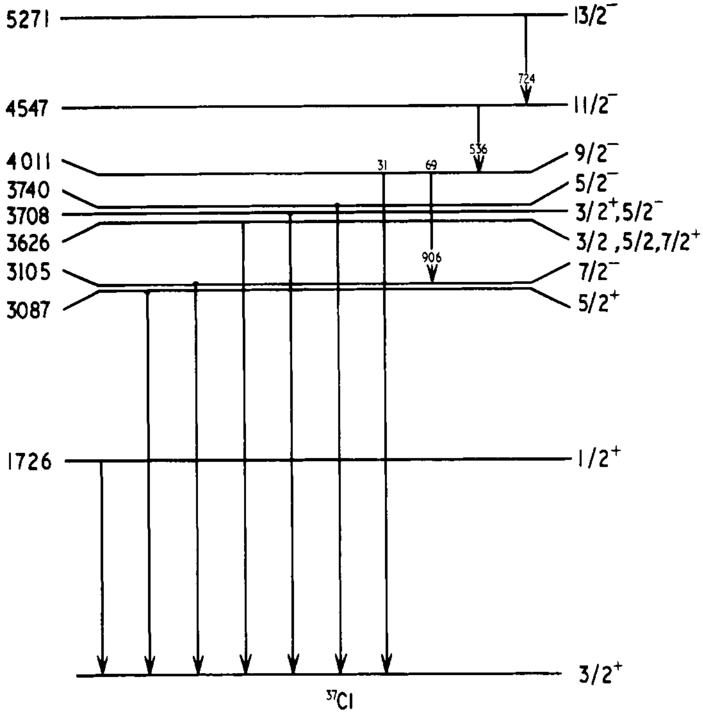

Figure 2. Decay scheme derived from the present work for levels in ^{37}Cl below 5·3 MeV excitation energy. The excitation energies on the left are in keV, the J^π values are given on the right.

gamma ray ($\tau = 48 \pm 5$ ps). The mixing ratio of the 3105 keV transition has previously been measured by Hyder *et al* (1969) using the ^{36}S(p, γ)^{37}Cl reaction not populating the 3087 keV level. These results, the statistical compound-nucleus reaction model predictions for the substate populations and the intensities at 90° and 110° have been used to calculate the intensity of the 3105 keV gamma ray at angles between 0° and 60°. This enables the intensity of the 3087 keV gamma ray to be found at these angles. The resulting angular distribution and chi-squared plots are shown in figure 3. The value of $\delta = -(1{\cdot}6 \pm 0{\cdot}4)$ is not in disagreement with the value found by Alenius *et al* (1972) (see table 5). This level must therefore have $J^\pi = \frac{5}{2}^+$ as negative parity would imply an M2 transition strength of greater than 250 Wu (Weisskopf single particle units) (Skorka *et al* 1966).

3.2. The 3626 keV, 3708 keV and 3740 keV levels

The 3740 keV level is strongly populated in the β decay of ^{37}S (Klotz and Walter 1973) implying negative parity. Our angular distribution and linear polarization data restrict the spin and parity to $\frac{3}{2}^+$ or $\frac{5}{2}^-$. Combining the two sets of data gives $J^\pi = \frac{5}{2}^-$. Little is known about the 3626 keV and 3708 keV levels from previous work. The spin and parity restrictions arising from the present work and the corresponding mixing ratios and transition strengths are given in table 4.

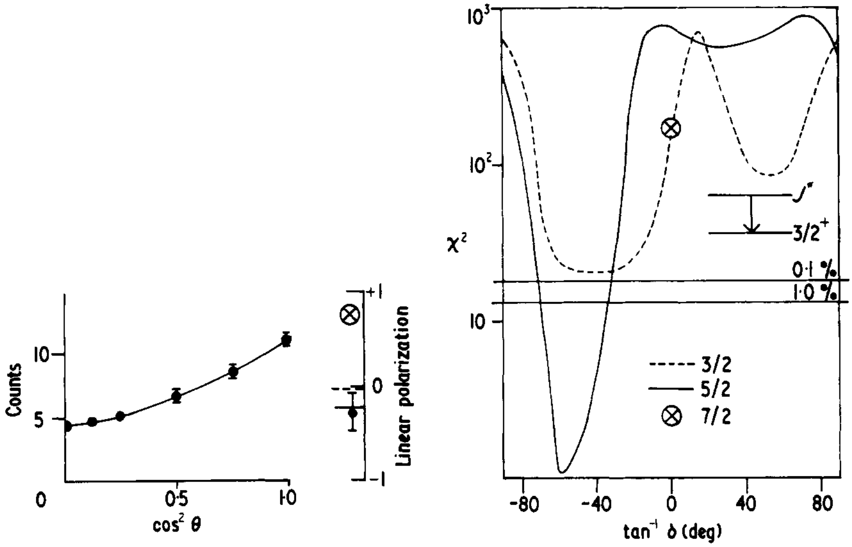

Figure 3. Angular distribution, linear polarization and χ^2 against $\tan^{-1}\delta$ plots for the 3087 keV gamma ray. The method used to extract the angular distribution has been given in the text and only the best fit is shown on the diagram. The linear polarizations corresponding to the minimum value of χ^2 for each spin hypothesis are shown by the appropriate symbol. The experimental linear polarization and its error are also shown in the diagram. The cross on the χ^2 plot indicates the value corresponding to $\delta = 0$ for the $\Delta J = 2$ transition. The spin $\frac{1}{2}$ hypothesis has $\chi^2 > 10^3$.

Table 5. Comparison of mixing ratios with those of Alenius *et al* (1972).

		δ	
E_x (keV)	E_γ (keV)	Present	Alenius *et al* (1972)
3087	3087	$-(1{\cdot}6 \pm 0{\cdot}4)$	-7^{+6}_{-24}
4011	906	$-(0{\cdot}73 \pm 0{\cdot}04)$	$-3{\cdot}5^{+0{\cdot}5}_{-0{\cdot}7}$
4547	536	$-(0{\cdot}04 \pm 0{\cdot}02)$	$2{\cdot}7^{+0{\cdot}8}_{-0{\cdot}6}$

3.3. The 4011 keV, 4547 keV and 5271 keV levels

Alenius *et al* (1972) using the same reactions as in the present work observed the decays of these three levels. However they wrongly attributed the 724 keV gamma ray to a decay from the 4011 keV level. Figure 4 shows part of the gamma-ray spectrum in coincidence with the 724 keV gamma ray. The appearance of the 536 keV and 906 keV gamma rays confirms our assignment. The 724 keV gamma ray is also found to have a threshold about 1·5 MeV above that of the 906 keV gamma ray. Figures 1(*b*), (*c*), (*d*) show the decay curves for the gamma rays from these three levels. The 906 keV and 3105 keV gamma rays were used as a check on the zero of the distance scale and once the zero had been established the decay curves for the 536 keV and 724 keV gamma rays were constrained to pass through the point $I_1/(I_1+I_2) = 1$ when $d = 0$. Figures 5, 6 and 7 show the angular distribution, linear polarization and chi-squared fits for these three levels. The spin and parity of the 4011 keV level are restricted to $\frac{9}{2}^-$ using the

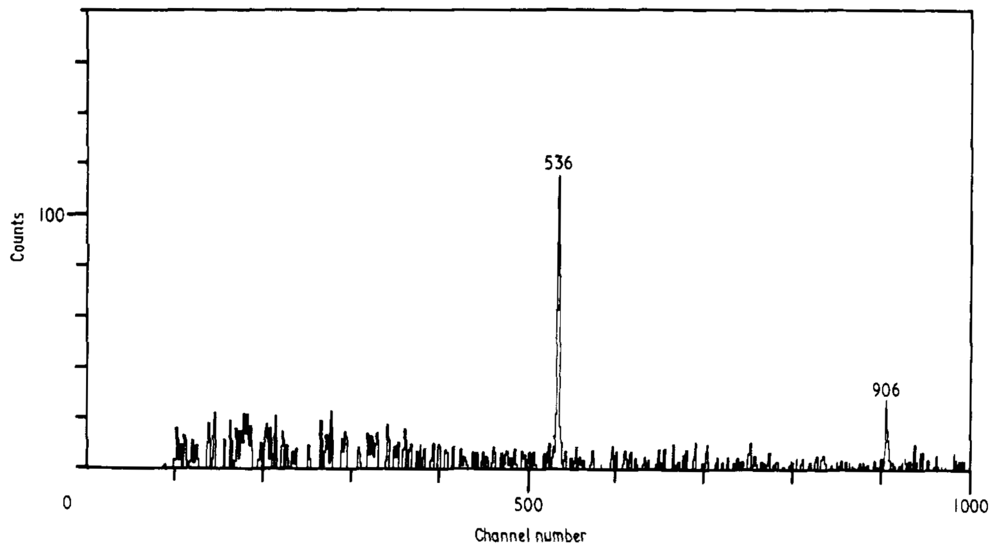

Figure 4. Part of the gamma-ray spectrum taken in coincidence with the 724 keV gamma ray showing the cascade 536 keV and 906 keV gamma rays. The dispersion is approximately 1 keV per channel.

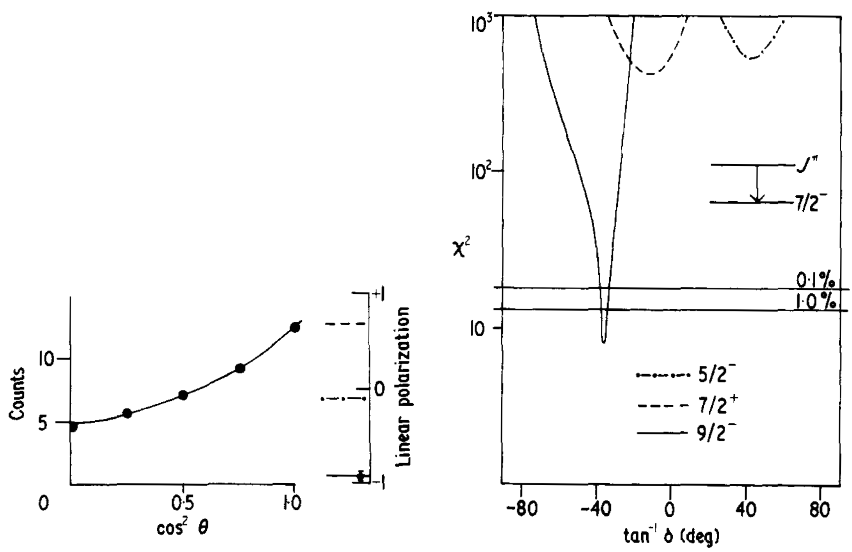

Figure 5. Angular distribution, linear polarization and χ^2 against $\tan^{-1}\delta$ plots for the 906 keV gamma ray from the 4011 keV level. An explanation of the diagram is given in the caption of figure 3. The spin hypotheses $\frac{3}{2}$ and $\frac{11}{2}$ have $\chi^2 > 10^3$.

measurements on the 906 keV transition (figure 5). The angular distribution data alone do not select definite spin values for the 4547 keV and 5271 keV levels. The linear polarization data however give definite spin and parity assignments for both levels as is indicated in figures 6 and 7. The mixing ratios we find disagree with those found by Alenius *et al* (1972) (see table 5). Their mixing ratio would give an E2 strength of 800 Wu for the 536 keV transition.

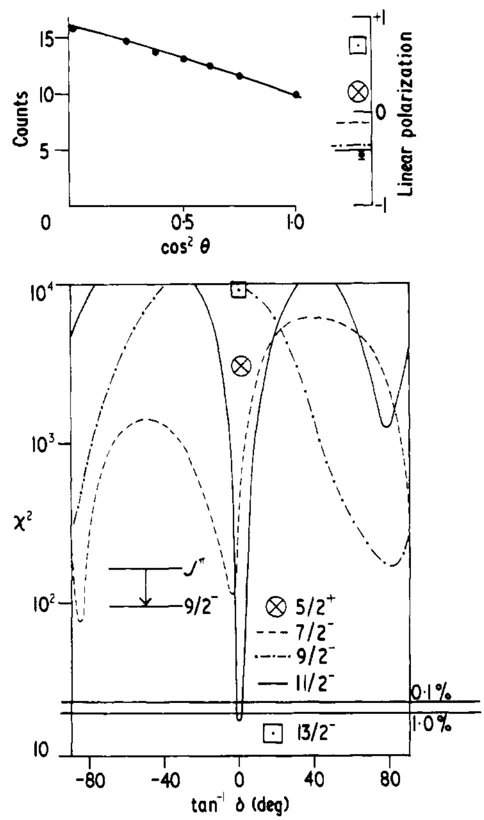

Figure 6. Angular distribution, linear polarization and χ^2 against $\tan^{-1}\delta$ plots for the 536 keV gamma ray from the 4547 keV level. The diagram is explained in the caption of figure 3. The cross and dot on the χ^2 plot are the values corresponding to $\delta = 0$ for the $\Delta J = 2$ transitions.

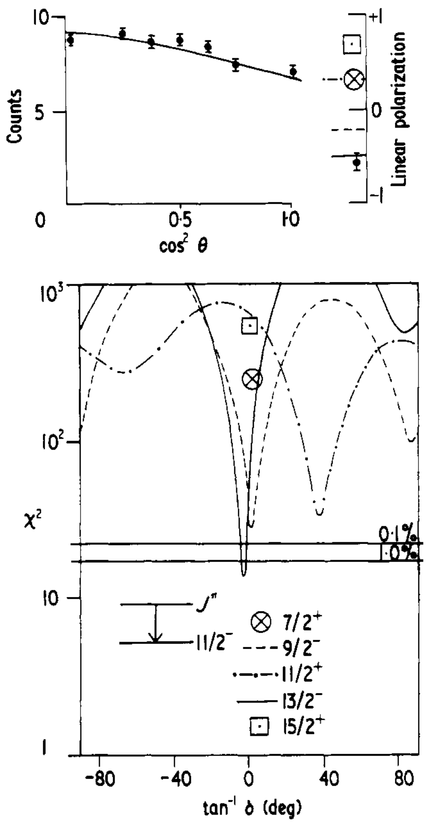

Figure 7. Angular distribution, linear polarization and χ^2 against $\tan^{-1}\delta$ plots for the 724 keV gamma ray from the 5271 keV level. The diagram and the symbols used are explained in the captions of figures 3 and 6.

4. Discussion

4.1. Positive-parity states

Shell-model calculations by Wildenthal *et al* (1971) predict three positive-parity states below 5 MeV. These are $\frac{1}{2}^+$, $\frac{3}{2}^+$ and $\frac{5}{2}^+$ at 1·67 MeV, 3·92 MeV and 3·28 MeV. These predictions compare well with the experimental values of 1·73 MeV and 3·09 MeV for the $\frac{1}{2}^+$ and $\frac{5}{2}^+$ states. There are two candidates for the $\frac{3}{2}^+$ level predicted by the shell model, these are the 3·63 MeV and 3·71 MeV levels. The predicted transition strengths of the ground-state decays are 1 Wu and 5 mWu for the E2 and M1 transitions respectively. Comparison with the experimental strengths given in table 4 shows good agreement for both levels.

4.2. Negative-parity states

Recent measurements in the upper region of the s–d shell have shown that the high-spin negative-parity states in ^{29}Si can be explained by the simple rotational model (Viggars *et al* 1973), while the core-excitation model can be applied successfully to the negative-parity states of ^{37}Ar (Gadeken *et al* 1974). In both of these models one of the main characteristics is that the states decay with large E2 transition strengths, about 25 Wu in ^{29}Si and about 10 Wu in ^{37}Ar. Table 4 shows that the largest E2 transition strength arising from the decay of a negative-parity state in ^{37}Cl is only about 1 Wu. Twin *et al* (1973) have reported four high-spin negative-parity levels in ^{35}Cl. These are $\frac{7}{2}^-$, $\frac{9}{2}^-$, $\frac{11}{2}^-$ and $\frac{13}{2}^-$ at 3162 keV, 4348 keV, 5408 keV and 6088 keV respectively. The decays of these levels are similar to those in ^{37}Cl having E2 transition strengths of about 1 Wu with two exceptions. The M1 transition strengths however are not similar to those found in ^{37}Cl.

A multiplet of negative-parity states has recently been found in ^{39}K (Durell *et al* 1974). These are explained as a $d_{3/2}$ hole weakly coupled to the 3^- state in ^{40}Ca. This gives four states with $J^\pi = \frac{3}{2}^-$ to $\frac{9}{2}^-$. The picture in ^{37}Cl is however less simple, states of this type can be made by coupling a $d_{3/2}$ hole to both the 3^- and 5^- states in ^{38}Ar giving a total of eight states. The 3^- and 5^- states occur at excitation energies of 3810 keV and 4585 keV so these configurations will probably mix. The 4547 keV ($\frac{11}{2}^-$) and 5271 keV ($\frac{13}{2}^-$) levels could arise from coupling a $d_{3/2}$ hole to the 5^- state. The M1 transition of 31 ± 5 mWu between these two levels is consistent with the value of about 10 mWu expected from the weak-coupling model. The 4011 keV ($\frac{9}{2}^-$) state could arise from either configuration. The E3 strength of the ground-state transition is 13 ± 1 Wu which is in good agreement with the ^{38}Ar ($3^- \rightarrow 0^+$) E3 transition strength of 16 ± 6 Wu.

Shell-model calculations using an inert ^{32}S core have been performed by Erné (1966) and Maripuu and Hokken (1970). Erné allowed one particle to be excited into

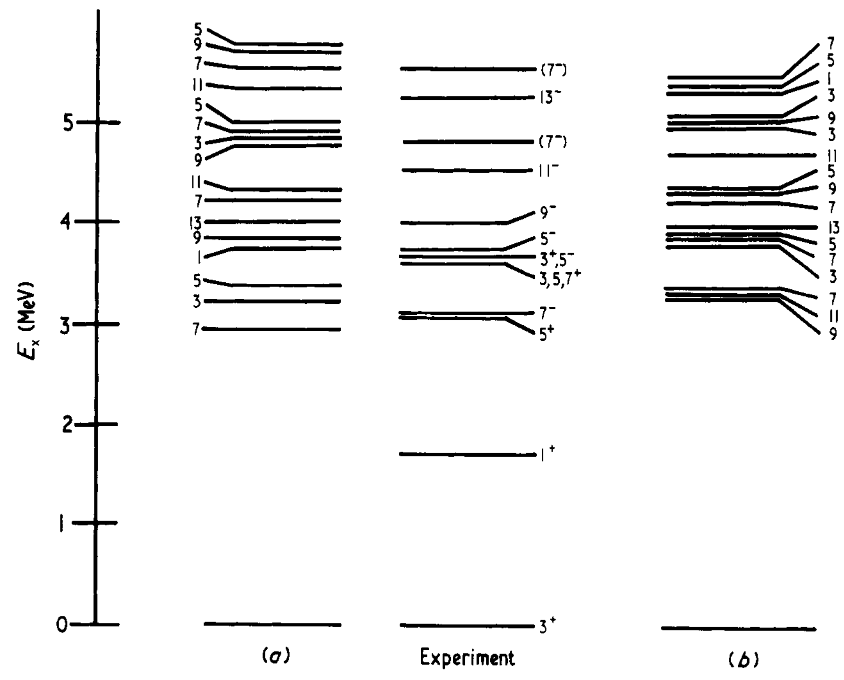

Figure 8. Comparison of the experimental level energies with those predicted by the shell model. The experimental levels come from the present work and that of Harris and Perizzo (1970). All the levels are labelled with $2J$ (ie 7 indicates $\frac{7}{2}$). The configurations used in the calculations are (*a*) $(d_{3/2})^4 f_{7/2}$ by Erné (1966), (*b*) $(d_{3/2})^4 f_{7/2}$ and $(d_{3/2})^4 p_{3/2}$ by Maripuu and Hokken (1970). Both calculations used an inert ^{32}S core.

the $1f_{7/2}$ orbital while the other calculation allowed one particle to be excited into either the $1f_{7/2}$ or the $2p_{3/2}$ orbital. Figure 8 shows a comparison between the calculated and the experimental energy levels below 5·5 MeV. The main feature is that the number of predicted levels in this region of excitation energy is much higher than that found experimentally. In particular the interaction used by Maripuu and Hokken (1970) predicts many high-spin states at low excitation energies. This is perhaps not surprising as the aim of the calculation was to predict the strengths of the analogue to anti-analogue M1 transitions and there was no experimental information on high-spin negative-parity states when the calculation was performed.

5. Conclusions

A detailed investigation of low-lying levels in ^{37}Cl has been completed. Shell-model calculations reproduce well the energies of the two known positive-parity states but they predict more low-lying negative-parity states than have been seen experimentally. The high-spin negative-parity states cannot be explained by the simple rotational model or the core-excitation model, but they have certain similarities with the high-spin negative-parity states of ^{35}Cl. Shell-model calculations allowing holes in the $1d_{5/2}$ and $2s_{1/2}$ shells and excitations into the $1f_{7/2}$ and $2p_{3/2}$ shells should have more success in explaining the negative-parity states of ^{37}Cl.

Acknowledgments

This work was supported by grants from the United Kingdom Science Research Council. Two of us (PJN and AJB) were the recipients of SRC postgraduate studentships during the period of this work. We thank Mr J B Reynolds for making the targets.

References

Alenius N G, Skeppstedt O and Wallander E 1972 *Phys. Scr.* **6** 303–8
Butler P A *et al* 1973 *Nucl. Instrum. Meth.* **108** 497–502
Camp D C and Meredith G L 1971 *Nucl. Phys.* A **166** 349–77
Duncan D D, Buerger K H, Place R L and Kern B D 1969 *Phys. Rev.* **185** 1515–27
Durell J L *et al* 1974 *Nucl. Phys.* A **219** 1–19
Endt P M and van der Leun C 1974 *Atomic Data and Nuclear Data Tables* **13** No 1
Erné F C 1966 *Nucl. Phys.* **84** 91–105
Gadeken L L *et al* 1974 *J. Phys.* A: *Math., Nucl. Gen.* **7** 83–99
Harris G I and Perizzo J J 1970 *Phys. Rev.* C **2** 1347–60
Hyder A K Jr, Harris G I, Perizzo J J and Kendziowski F R 1969 *Phys. Rev.* **169** 899–910
James A N, Twin P J and Butler P A 1974 *Nucl. Instrum. Meth.* **115** 105–13
Klotz G and Walter G 1973 *Phys. Rev.* C **7** 854–5
Maripuu S and Hokken G A 1970 *Nucl. Phys.* A **141** 481–92
Nichols D B, Kern B D and McEllistrem M T 1966 *Phys. Rev.* **151** 879–86
Nolan P J *et al* 1973 *J. Phys.* A: *Math., Nucl. Gen.* **6** L37–40
Piiparnen M, Vitasalo M and Anttila A 1973 *Phys. Scr.* **8** 236–8
Sharpey-Schafer J F *et al* 1973 *Proc. Int. Conf. on Nuclear Physics, Munich* (Amsterdam: North Holland) p 283
Skorka S J, Hertel J, Retz-Schmidt T W 1966 *Nucl. Data* A **2** 347
Twin P J *et al* 1973 *Proc. Int. Conf. on Nuclear Physics, Munich* (Amsterdam: North Holland) p 170
Viggars D A *et al* 1973 *J. Phys.* A: *Math., Nucl. Gen.* **6** L67–72
Wildenthal B H, Halbert E C, McGrory J B and Kus T T S 1971 *Phys. Rev.* C **4** 1266–314